Received: 4 May 2020 | Revised: 8 October 2020 | Accepted: 15 October 2020

DOI: 10.1002/dep2.130

ORIGINAL RESEARCH ARTICLE

The Depositional Record Open Access
A journal of the International Association of Sedimentologists
WILEY

Holocene progradation and retrogradation of the Central Texas Coast regulated by alongshore and cross-shore sediment flux variability

Christopher I. Odezulu[1] | **Travis Swanson**[2] | **John B. Anderson**[1]

[1]Department of Earth, Environmental and Planetary Science, Rice University, Houston, TX, USA

[2]Department of Geology and Geography, Georgia Southern University, Statesboro, GA, USA

***Correspondence**
Christopher I. Odezulu, Department of Earth, Environmental and Planetary Science, Rice University, Houston, TX, USA.
Email: ikodezulu@yahoo.com

Funding information
Rice University Shell Center for Sustainability.

Abstract

Fifteen transects of sediment cores located off the central Texas coast between Matagorda Peninsula and North Padre Island were investigated to examine the offshore record of Holocene evolution of the central Texas coast. The transects extend from near the modern shoreline to beyond the toe of the shoreface. Lithology, grain size and fossil content were used to identify upper shoreface, lower shoreface, ebb-tidal delta and marine mud lithofacies. Interpretations of these core transects show a general stratigraphic pattern across the study area that indicates three major episodes of shoreface displacement. First, there was an episode of shoreface progradation that extended up to 5 km seaward. Second, an episode of landward shoreline displacement is indicated by 3–4 km of marine mud onlap. Third, the marine muds are overlain by shoreface sands, which indicates another episode of shoreface progradation of up to 5 km seaward. Radiocarbon ages constrain the onset of the first episode of progradation to *ca* 6.5 ka, ending at *ca* 5.0 ka when the rate of sea-level rise slowed from an average rate of 1.6–0.5 mm/yr. Results from sediment budget calculations and sediment transport modelling based on reasonable estimates of an ancient shoreline shape and wave climate indicate that the first progradation was a result of sand supplied from erosion of the offshore Colorado and Rio Grande deltas. The transgressive phase occurred between *ca* 4.9 ka and *ca* 1.6 ka and coincided with a major expansion of the Texas Mud Blanket, which resulted in burial of offshore sand sources and the shoreface being inundated with mud. The second, more recent episode of shoreface progradation began *ca* 500 years ago with a maximum rate of *ca* 6 m/yr. This most recent change signals a healing phase of coastal evolution from the late Holocene transgressive event. Currently, the shoreline along the central Texas coast is retreating landward at an average rate of 0.30 m/yr, indicating that the second progradation event has ended.

KEYWORDS

Central Texas, cross-shore sediment flux, longshore sediment flux, progradation, retrogradation, sea level, Texas Mud Blanket

This is an open access article under the terms of the Creative Commons Attribution License, which permits use, distribution and reproduction in any medium, provided the original work is properly cited.
© 2020 The Authors. *The Depositional Record* published by John Wiley & Sons Ltd on behalf of International Association of Sedimentologists.

1 | INTRODUCTION

Barrier islands and peninsulas dominate the Texas Coast. These coastal barriers are known to have had very different evolutionary histories during the Holocene (Anderson et al., 2014; Rodriguez et al., 2001). The main factors that influenced coastal change over this time interval include variability in antecedent topography, relative sea-level change, variable sediment supply, changes in surface current patterns, wave climate and storm history.

The central Texas Coast occupies a shelf embayment between the ancestral Colorado and Rio Grande deltas (Figure 1). The Holocene evolution of coastal barriers situated off the central Texas coast has been a focus of numerous investigators (Anderson et al., 2014; Garrison et al., 2010; McGowen et al., 1977; Morton, 1977; Shideler, 1986; Simms et al., 2006; Wilkinson, 1975; Wilkinson & Basse, 1978; Wilkinson & McGowen, 1977). These studies focussed on onshore records, which do not allow observations of shoreface progradation and retrogradation and where pristine material needed for radiocarbon dating is limited.

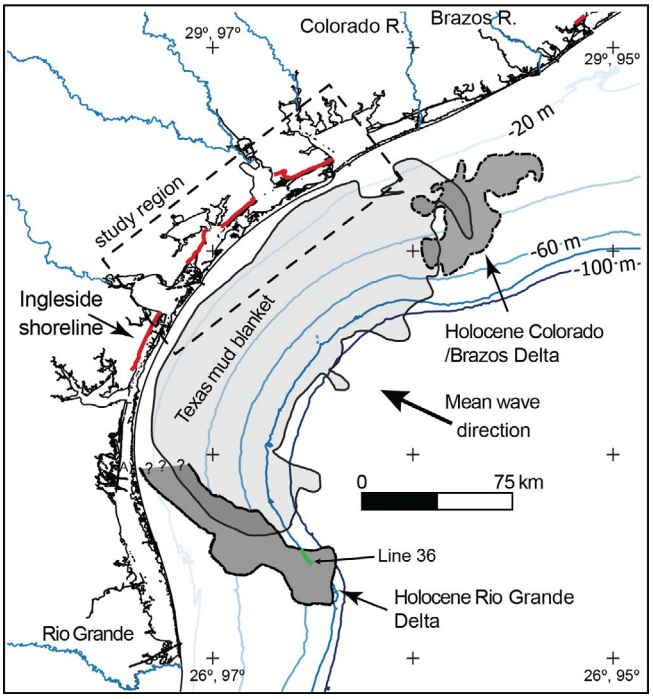

FIGURE 1 Map of the study area (dashed boxed region). Ingleside palaeo-shoreline is drawn as a thick red line. Depth along the continental shelf is contoured at a 20 m interval as indicated by blue contour lines. Also shown are the locations of the ancestral Colorado and Rio Grande deltas (mapped as dark grey regions; from Snow, 1998; van Heijst et al., 2001 and Banfield & Anderson, 2004, respectively) and the Texas Mud Blanket (mapped as light grey region; from Weight et al., 2011). Seismic line 36 is drawn as a green line along the Holocene Rio Grande Delta. Note that only the northern portion (US portion) of the Rio Grande Delta has been mapped.

Rodriguez et al. (2001) conducted research on sediment cores from the shoreface and inner continental shelf off the central Texas coast (Figure 2) and recognised different stages of shoreface growth and retreat, but lacked radiocarbon age constraints on the timing of these changes. The results from a more detailed analysis of the cores studied by Rodriguez et al. (2001) are presented here, including a revised facies and stratigraphic analysis that relies heavily on grain size as an indicator of depositional environment (Figure 3). In addition, radiocarbon ages provide constraints on key stratigraphic surfaces (Table 1). There are also the results from more recent studies of central Texas coastal barriers (Anderson et al., 2014; Garrison et al., 2010; Simms et al., 2006) and by Weight et al. (2011), who conducted a detailed investigation into the evolution of the Texas Mud Blanket (TMB), to examine the causes of coastal change in the study area.

2 | STUDY AREA

The offshore study area covers about 12,000 km^2 (shoreface to inner shelf) and extends from Matagorda Island southwards to North Padre Island (Figure 2). The continental shelf is an embayment characterised by a relatively steep, ramp-like profile that is bounded to the north by the ancestral Colorado Delta and to the south by the ancestral Rio Grande Delta (Figure 1). Shoreface profiles vary across the study area in response to changes in the antecedent topography and associated changes in the thickness of Holocene shoreface deposits (Figure 4).

The central Texas coast is a wave-dominated, micro-tidal environment. Tides are diurnal or mixed and have an average range of less than 60 cm (Morton et al., 2004). South-easterly winds are prevalent most of the year, with prevailing longshore currents towards the west in the northern sector and towards the north along the north-south oriented south Texas coast. Thus, despite the limited sand delivery from central Texas rivers, sand supply by longshore transport is relatively high for the central Texas coast compared to the upper Texas coast and south Texas coast (Curray, 1960; Lohse, 1955; McGowen et al., 1977).

Texas has one of the longest aerial photographic records of historical shoreline change in the United States, dating back to the late 1930s in some areas. For more than four decades, these data have been used to analyse historical shoreline change (Gibeaut et al., 2006; Morton, 1977; Paine et al., 2012; 2016). These results show that 84% of Texas coastal barriers are currently experiencing shoreline retreat, whereas 16% are experiencing shoreline advance (Paine et al., 2016). The most recent reviews of these data show that shoreline change varies spatially and temporally along the coast, with shoreline landward retreat rates ranging from 0.5 to 5.5 m/

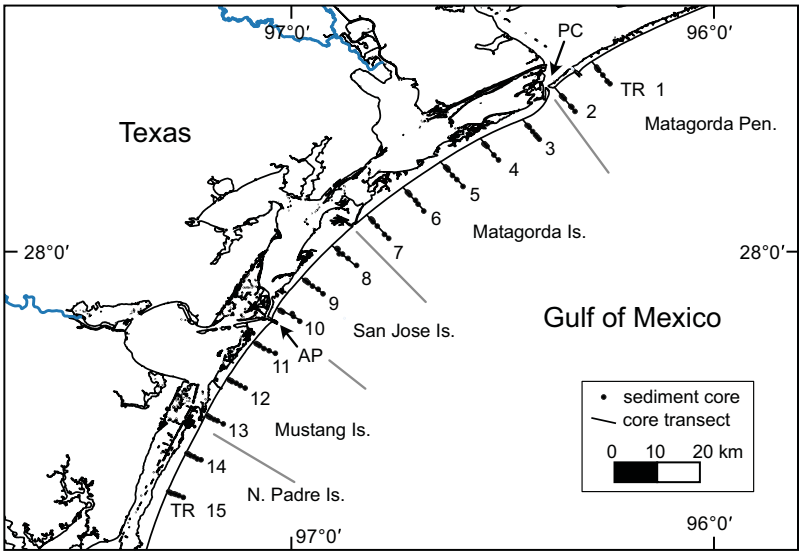

FIGURE 2 Locations of sediment core transects used for this study. Aransas Pass and Pass Cavallo are annotated by labels AP and PC, respectively

yr and averaging *ca* 1.6 m/yr along the upper Texas coast, 0.30 m/yr in central Texas and *ca* 1.9 m/yr in south Texas (Gibeaut et al., 2006; Paine et al., 2012). Comparisons of these rates to the pre-historic record of coastal change have shown that current rates along the upper and south Texas coast are unprecedented, a result of diminished sand supply, accelerated sea-level rise and anthropogenic influences (Anderson et al., 2014; Odezulu et al., 2018; Wallace & Anderson, 2013).

Historic rates of relative sea-level rise, based on tide gauge records, vary along the Texas coast from 6.4 mm/yr at east Galveston Island to 2.1 mm/yr at Port Mansfield on South Padre Island (NOAA Tides & Currents, 2012). These differences are due to variations in glacial isostatic-adjustment, local steric changes, local oceanographic influences and subsidence (Kolker et al., 2011; Morton et al., 2006; Paine, 1993; Paine et al., 2012; Simms et al., 2007; 2013). Variations in subsidence are primarily related to differences in the thickness and degree of compaction of Holocene sediments, which ranges from *ca* 1 to 50 m along the coast; thicker accumulations are associated with incised valleys (Anderson et al., 2014).

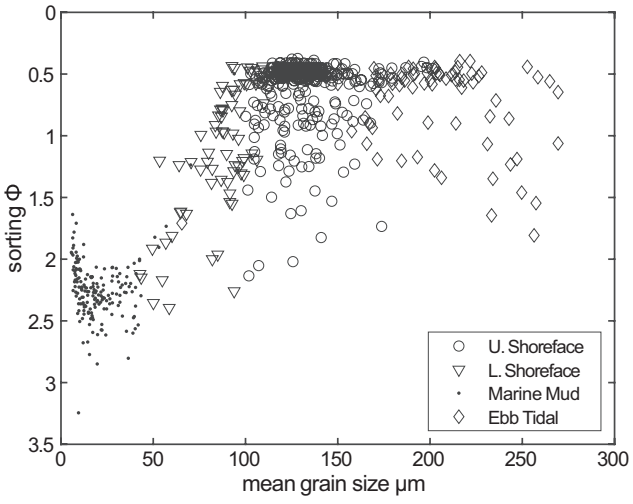

FIGURE 3 Sorting (Φ) as a function of mean grain size (μm) for sampled portions of interpreted lithofacies: upper shoreface (open circles), lower shoreface (triangles), marine mud (dots) and ebb-tidal (diamonds)

2.1 | Early Evolution of the Central Texas Coast

During the MIS (marine isotope stage) 5e highstand, the Texas shoreline was situated approximately 30 km landward of the modern shoreline along the upper Texas coast, but about half that distance from the modern central Texas shoreline (Ingleside palaeo-shoreline, shown as a thick red line in Figure 1; Otvos & Howat, 1996; Simms et al., 2013). The MIS 5e highstand was followed by more than 100 m of episodic sea-level fall when the ancestral Brazos, Colorado and Rio Grande rivers formed large fluvial-dominated deltas on the continental shelf (Abdulah et al., 2004; Banfield & Anderson, 2004). The central Texas shelf was situated between these deltas and there the shoreline prograded seaward until the end of MIS 3 time, when the rate of sea-level fall increased, outpacing the progradation of the shoreline (Eckles et al., 2004). During the Stage 2 sea-level lowstand, rivers and streams eroded the exposed continental shelf creating the irregular Pleistocene surface on which Holocene coastal systems were established (Anderson et al., 2014; Simms et al., 2007). During the initial late Pleistocene–Early Holocene flooding of the outer continental shelf, the palaeo-shoreline migrated rapidly landwards, but little is known about coastal evolution at this time because coastal deposits of this age are buried beneath the TMB (Weight et al., 2011). The exception is coralgal reefs on the mid-shelf with prominent terraces that record punctuated sea-level rise during this time interval (Khanna et al., 2017).

TABLE 1 Radiocarbon age date information

Core ID	Lab number	Location	Latitude°	Longitude°	Material	F Modern	Fm Error	Depth (cm)	Uncalibrated age (year)	Age error (±year)	Δ13C	2σ calibrated 14C yr BP start	2σ calibrated 14C yr BP end
TR 11-76	148572	Mustang Island	27.7655	97.05667	Mulinia	1.11840	0.00270	33	Modern	—	−0.42	—	—
TR 11-76	148583	Mustang Island	27.7655	97.05667	Art. Chione Cancellata	0.70220	0.00160	180	2,840	20	1.38	2,500	2,698
TR 12-82	148573	Mustang Island	27.68717	97.13433	Peristichia toreta	0.94270	0.00240	130	475	20	−01	0	221
TR 12-83	148574	Mustang Island	27.68133	97.1245	Mulinia	0.40110	0.00130	75	7,340	25	0.79	7,719	7,894
TR 13-89	148575	Mustang Island	27.599	97.186	Mulinia	0.44820	0.00150	70	1970	20	—	1,441	1,602
TR 13-89	148576	Mustang Island	27.599	97.186	Gastropod	0.78250	0.00190	230	6,450	25	0.1	6,844	7,030
TR 14-95	148577	N. Padre Island	27.51167	97.24067	Olivia	0.82310	0.00190	240	1,560	20	0.5	1,044	1,201
TR 15-103	148578	N. Padre Island	27.41783	97.27933	Mulinia	1.16560	0.00270	85	Modern	—	0.31	—	—
TR 15-104	148579	N. Padre Island	27.41583	97.274	Peristichia Toreta	0.54680	0.00160	330	4,850	25	1.77	5,042	5,264

Note: Quantities not measured by the laboratory are indicated by a dash (—).

Starting at approximately 11.5 ka, both the Rio Grande and the Colorado rivers again constructed large deltas on the inner shelf (Banfield & Anderson, 2004; Snow, 1998; Figure 1). Both the Colorado and Rio Grande deltas rest on the MIS 2 sequence boundary (Figure 5), but only the Colorado Delta has yielded radiocarbon ages to constrain its early Holocene age. The age of the Rio Grande Delta is loosely constrained by water depths and the sea-level curve for the region (Livsey & Simms, 2013; Milliken et al., 2008). Both deltas exhibit clinoforms whose thickness and variable orientations indicate lobe shifting (e.g. Figure 5), which combined with detailed mapping indicates that they were fluvial-dominated deltas (Banfield & Anderson, 2004; Snow, 1998).

Both the Colorado and Rio Grande deltas were eroded during transgression, removing topset strata entirely and truncating foreset beds (e.g. Figure 5). Both deltas changed from strongly lobate fluvial-dominated deltas to shore-aligned deltas that lack clinoforms during their final stages of development, indicating a change to wave-dominated deltas (Banfield & Anderson, 2004; Snow, 1998). These wave-dominated deltas are situated to the north (Rio Grande) and north-east (Colorado) of their fluvial-dominated predecessors (Figure 1), indicating longshore sediment transport in that direction. Based on their depths and locations, these wave-dominated deltas began to form at *ca* 9.5 ka. At the same time these wave-dominated deltas were active, the shoreline in the vicinity of Mustang Island was near its current location (Simms et al., 2006), indicating that a deep coastal and shelf embayment existed at this time. Throughout the Holocene, the embayment has been filled with up to 50 m of marine mud of the TMB (Shideler, 1978). The most rapid growth of the TMB occurred during the late Holocene when its volume increased by *ca* 172 km^3, more than doubling its size and thickness within 3.5 ka (Weight et al., 2011). Most of this sediment came from the Mississippi River, with contributions from the Rio Grande and Brazos/Colorado rivers, and the flux of sediment is believed to have been regulated by changes in circulation in the Gulf (Weight et al., 2011).

3 | METHODOLOGY

The nearshore core collection used for this study consists of 15 transects, each with seven 1–5 m long pneumatic hammer cores (Figure 2) that were collected during the Summer of 1997 (Fassell, 1999). The transects extend from the upper shoreface, from approximately 2 m water depth to the inner shelf in water depths of between 12 and 14 m. During the Summer of 2016, four additional cores were acquired from the beach and upper shoreface, in *ca* 1 m water depth, off the western part of Mustang Island and North Padre Island. After collection, all cores were halved. One half was logged

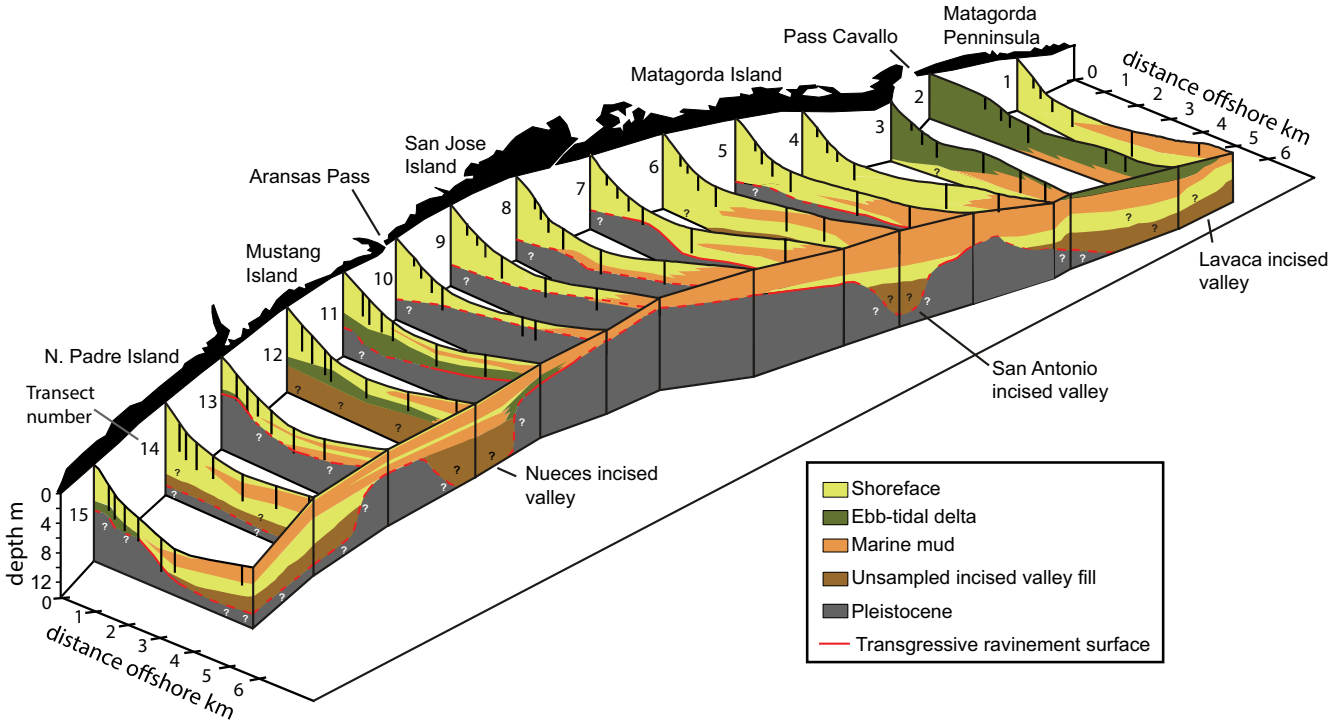

FIGURE 4 Regional lithofacies map of the study area showing cores sampled for radiocarbon date and their ages. Note that thickness and stratigraphy of sampled sections vary in response to the depth to the Pleistocene surface. Note also that upper and lower shoreface lithofacies are combined here to emphasise progradation and retrogradation events. Modified from Rodriguez et al. (2001)

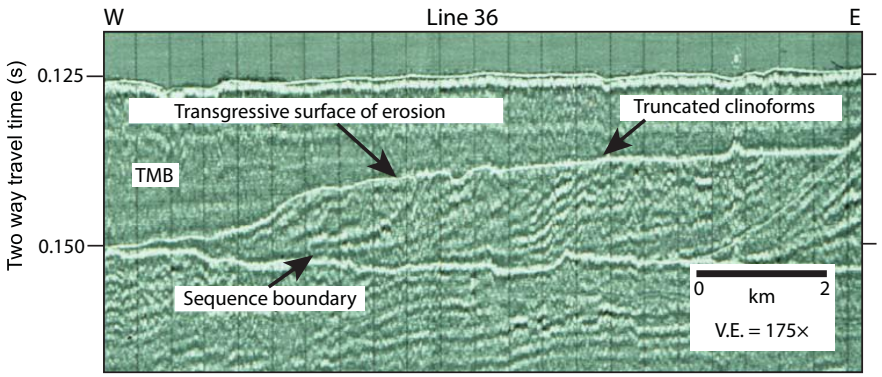

FIGURE 5 Seismic line 36 from Banfield and Anderson (2004) shows the transgressive surface of erosion (i.e. transgressive ravinement surface) and onlap of the Texas Mud Blanket (TMB). The package of delta clinoforms shows variable dip angles, which are interpreted to represent lobe extension from various distributary channels of a fluvial-dominated delta. These clinoforms are truncated by the transgressive surface of erosion. The location of line 36 is shown as a green line in Figure 1

shortly after acquisition for lithology, fossil content and sedimentary structures by Fassell (1999). This study is based on new logs and interpretations performed using the preserved halves.

A Malvern Mastersizer 2000 laser particle size analyser was used to carry out grain size analyses. The instrument utilises laser diffraction in sediment suspended in water to obtain measurements. The typical sampling interval varied depending on down-core lithological variability; being 20 cm for lower shoreface and inner shelf cores and 50 cm for nearshore cores that sampled dominantly sand.

A total of nine monospecific mollusc shells (mainly *Mulinia* and various gastropod shells), retrieved from seven different cores, were radiocarbon dated at the Woods Hole Oceanographic Institution's Mass Spectrometer (AMS) facility (Table 1). The radiocarbon dates were calibrated using the Calib. Rev. 7.10 program (Reimer et al., 2013), using the standard 400 year marine reservoir correction based on results from Milliken et al. (2008).

4 | RESULTS

4.1 | Lithofacies

Lithofacies analysis was initially conducted on all 15 core transects and used to correlate lithofacies between core transects (Fassell, 1999; Rodriguez et al., 2001; Figure 4). These lithofacies correlations build on the earlier results using a new, more robust grain size dataset (Figure 3). The earlier stratigraphic framework has been modified based on the revised lithofacies classification presented here (Figure 4). Upper and lower shoreface lithofacies were combined in Figure 4 so that progradation and retrogradation events are easily visualised.

Upper Shoreface sands consist of well-sorted, fine sand. Thin muddy sand/sandy mud interbeds are rare. Mean grain size ranges from 110 to 170 μm (Figure 3). Shells are common, including the genera *Mulinia* and *Donax*. Shell hash and shell lags are present, but bioturbation is rare. Lower shoreface facies consist of muddy sand to sandy mud. The mean grain size ranges from 50 to 110 μm (Figure 3). Gastropod and Pelecypod shells occur sparsely and bioturbation is common. *Skolithos* traces are most common among the ichnofauna. Marine mud is brownish to light gray in colour and characterised by abundant benthic foraminifera and shells, including gastropods with *Olivia* sp. and *Peristichia toreta* being the most common. The mean grain size is predominantly less than 50 μm (Figure 3). This lithofacies extends from the toe of the shoreface to the inner continental shelf.

Inlet/ebb-tidal facies are predominantly medium to fine sands. Shell hash and shell lags are common. The mean grain size ranges from 150 to 270 μm (Figure 3). This facies was sampled in the top portions of transects 2 and 3, which are located offshore present-day Pass Cavallo, and in transects 11, 12 and 15, which were collected offshore Mustang and North Padre islands, where it is buried beneath shoreface sands (Figure 1).

Several cores bottomed-out in Pleistocene sediments. These Pleistocene sediments are compacted and often oxidized olive-brown clayey sand with isolated carbonate concretions. Pleistocene sediments were sampled in cores transects 15, 10, 9, 8, 7 and 5, which are situated on antecedent highs associated with interfluves (Figure 4).

4.2 | Stratigraphy

Rodriguez et al. (2001) noted a regionally consistent pattern of shoreface progradation and retrogradation across the central Texas shelf that is best preserved in core transects collected within offshore incised valleys of the ancestral Lavaca, San Antonio and Nueces rivers (Figure 4). Condensed and incomplete stratigraphic sections were acquired in transects collected on Pleistocene highs located offshore of western San Jose Island and the northern end of North Padre Island. The general stratigraphy recorded in the core transects includes two episodes of shoreface progradation that are marked by sand units that fine offshore from fine to very fine sand separated by marine mud. The early progradation resulted in shoreface sands and ebb-tidal delta sands that extend just over 5 km seaward of the current shoreline (Figure 6). Marine mud directly overlies this lower sand unit, indicating an approximately 3 km retreat of the shoreface. The second phase of shoreface progradation extended between 2 and 5 km from the current shoreline.

Core transects TR 2, 3, 11, 12 and 15 sampled relatively coarse (170–270 μm) sand with shell debris layers interpreted as inlet and ebb-tidal delta deposits (Figures 4 and 6). Modern ebb-tidal delta deposits were sampled only in Transect 2 and 3 offshore of the current Pass Cavallo tidal inlet. Older ebb-tidal delta sands occur within the lower progradational unit offshore of Mustang Island and North Padre Island and record previous locations of tidal deltas. While no modern ebb-tidal delta deposits were sampled west of Pass Cavallo, tidal deposits compose a major portion of Mustang Island (Simms et al., 2006).

4.3 | Radiochronology

Nine samples from core transect TR 11 through TR 15 were used for radiocarbon dating the two progradational events and single flooding event identified in the core transects (Figure 6; Table 1). The oldest sample age (*ca* 7,340 ± 25 cal BP) was obtained from a *Mulinia* shell collected from the lower progradational ebb-tidal delta unit at the base of core TR 12-83. The exact lithological context for each sample location is given in Figure 6 annotated ages. Cores from transect 11 sampled this same unit. Both core transects were collected within the Nueces incised valley and indicate that an ebb-tidal delta occupied this portion of the valley at this time. These results are consistent with those of Shideler (1986) and Simms et al. (2006) indicating that Mustang Island was located at or near its current location at this time.

Drill cores from the southern part of Corpus Christi Bay sampled flood tidal delta deposits that are correlated to the offshore ebb-tidal delta deposits; radiocarbon dates from these deposits range in age from *ca* 6.5 ka to Modern (Simms et al., 2006). The lower portion of these flood tidal delta deposits extends *ca* 6 km north of the current bayline. Thus, this ancestral tidal delta complex was significantly larger than the modern Port Aransas tidal delta complex, consistent with greater sand supply to the coast at this time. Likewise, a drill core from Matagorda Bay sampled flood tidal delta deposits that range in age from *ca* 7.4 to 6.7 ka and record a

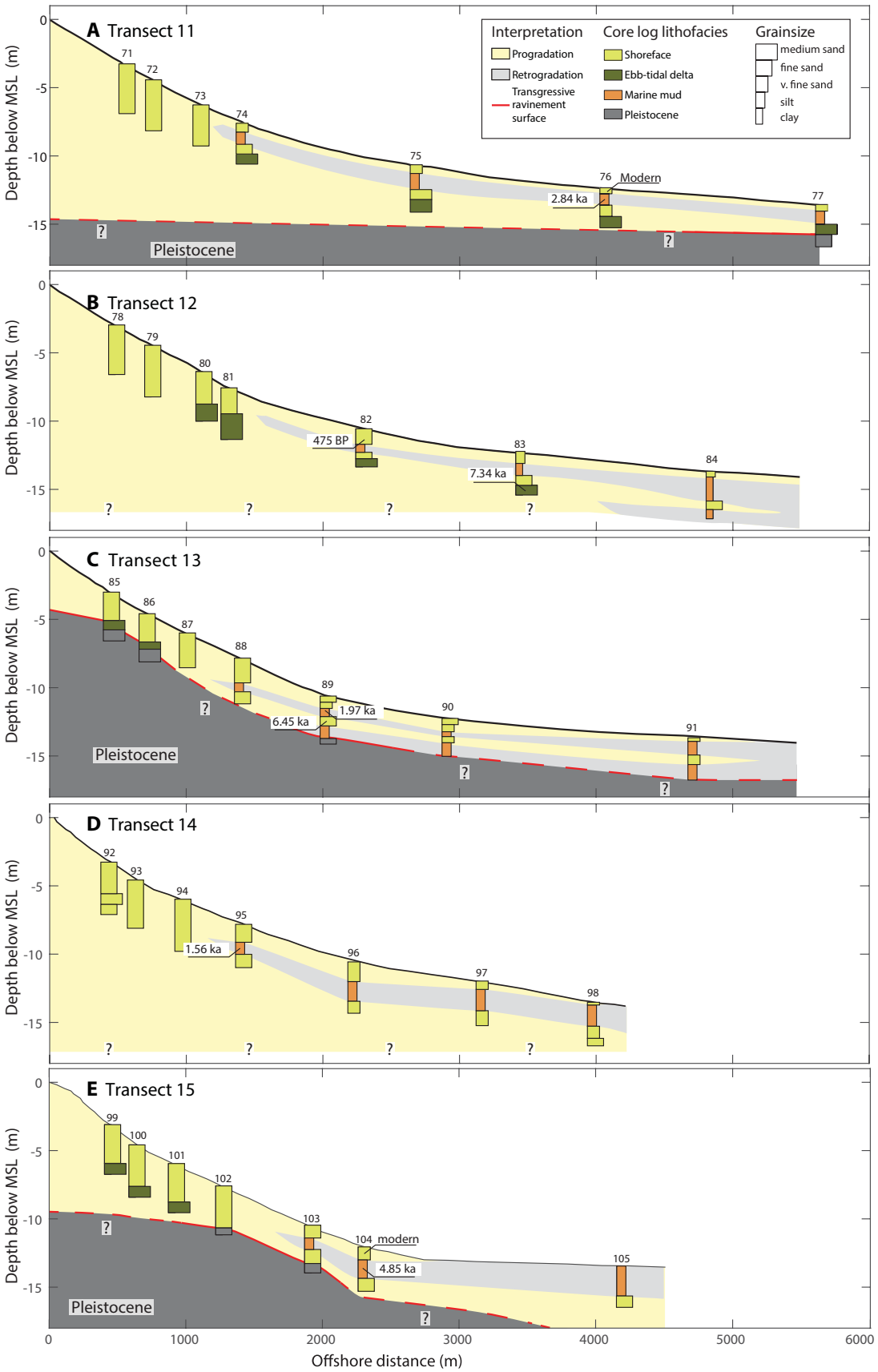

FIGURE 6 Lithologic logs, grain sizes and ages for core transects (A) 11, (B) 12, (C) 13, (D) 14 and (E) 15, which sampled the most expanded stratigraphic sections and record two episodes of shoreface progradation separated by onlap of marine mud. Radiocarbon ages are also shown (see Table 1 for details)

time when the tidal delta was larger than at present (Maddox et al., 2008).

Above the ebb-tidal delta unit sampled in transects 11 and 12 is a fine to very fine shoreface sand that extends across the study area, with the exception of core transects collected on antecedent highs offshore of San Jose Island and North Padre Island (Figures 2 and 4). The onset of this lower shoreface-progradation event is constrained to *ca* 6,450 ± 25 cal BP by a date from a gastropod shell collected from TR13-89 (Figure 6C). Thus, the older progradational event was underway by *ca* 7.3 to 6.5 ka and coincided with the construction of large tidal delta complexes in Matagorda and Corpus Christi bays.

The older shoreface-progradation event culminated with marine mud onlap of shoreface sands (Figures 4 and 6). A radiocarbon age from a *Peristichia toreta* shell from the marine mud unit in Core TR15-104 yielded a radiocarbon age of 4,850 ± 25 cal BP and is used to constrain the onset of mud onlap (Figure 6E). Additional age constraints for marine mud onlap comes from an *Oliva* shell from core TR14-95 that yielded an age of 1,560 ± 20 cal BP, a *Mulinia* shell from TR13-89 of 1970 ± 20 cal BP, and an *articulated Chione cancellata* shell from TR 11-76 that yielded an age of 2,840 ± 60 yr BP (Figure 6A, C and D). These combined ages indicate that mud onlap of the shoreface was underway by 4,850 ± 25 cal yr BP and ended after 1,560 ± 20 cal yr BP.

The final stage of shoreface progradation is recorded by a thin (<1 m), shoreface unit that extends *ca* 5 km seaward of the current shoreline (Figures 4 and 6). Radiocarbon dates from Core TR14-95 indicate that this most recent progradation occurred soon after the *ca* 1.5 ka transgression and continued into modern time (Figure 6D). This is supported by three other radiocarbon dates from the youngest progradational unit that range from 475 ± 20 cal BP from a *Peristichia toreta* shell from Core TR 12-82 and two modern dates from above this surface in cores TR 11-76 and TR15-103 (Figure 6A,B and E).

4.4 | Sediment Budget Analysis

The sediment cores show a history of significant shoreface progradation and retrogradation that was controlled by both sand and mud supply to the coast. Fluvial sand supply to the central Texas coast was from the Brazos, Colorado and Rio Grande rivers; other rivers of central Texas flow into bays where most of the sand is sequestered in bayhead deltas. The other major source of sand to the area comes from the erosion of the offshore Brazos, Colorado and Rio Grande deltas. This is based on seismic records that show truncation of topset and foreset beds in these deltas (Abdulah et al., 2004; Banfield & Anderson, 2004; Snow, 1998; van Heijst et al., 2001) (Figure 5).

Previous studies along the Texas coast have shown that transgressive ravinement occurs at water depths of 8–10 m, which generally coincides with the physiographic toe of the shoreface (Rodriguez et al., 2001; Siringan & Anderson, 1994; Wallace & Anderson, 2010). Assuming a similar depth of ravinement during the Holocene transgression, Anderson et al. (2014) calculated that as much as 36.6 km^3 of sand could have been eroded from the offshore Brazos, Colorado and Rio Grande deltas. Much of this sand is thought to reside in offshore valleys and storm beds. A total sand volume of 10 ± 3 km^3 is estimated to exist within the modern barrier island systems of the central Texas coast, based on data from, Matagorda Peninsula (Wilkinson & McGowen, 1977), Matagorda Island (Wilkinson, 1975), San José Island (Anderson et al., 2014), Mustang Island (Simms et al., 2006), and North and South Padre islands. Based on offshore data (Figure 4), the thickness of shoreface sands is estimated to vary between *ca* 10 m (typical thickness) and *ca* 1.5 m (in isolated regions between incised valleys). A rough, yet plausible estimate of modern shoreface sand volume can be made by multiplying the typical maximum shoreface sand thickness of *ca* 10 m by the observed shoreface progradation distance of *ca* 5 km and the *ca* 200 km alongshore distance of the study area. This coarse estimate of shoreface sand volume yields *ca* 10 km^3**;** therefore when combined with the volume of the modern barriers, in terms of an order-of-magnitude estimate, this approximated sand budget roughly balances. However, to further test the hypothesis that shoreface progradation along the central Texas coast was driven by longshore transport from updrift deltaic headlands, the possible rates of longshore sediment fluxes are explored using a simple numerical model.

4.5 | Modelling Results

A forward model of shoreline motion due to longshore sediment transport is applied to explore the wave-reworking of the Brazos-Colorado and Rio Grande deltaic systems and convergence of longshore sediment transport along the Central Texas coast (Figure 1). The aim of the modelling component of this study is to conduct a conceptual check to see if reasonable approximations of palaeo-shoreline shape and ancient wave climate could explain longshore convergence of sediment transport to drive over 5 km of shoreline progradation over a period of *ca* 2 ka observed along the central Texas coast (Figures 4 and 6).

To initialise the simulation, closest-in-time palaeogeographic reconstructions of the Central Texas coast are used (Figure 1). These reconstructions rely on published reconstructions of the Brazos and Colorado (Abdulah et al., 2004; Snow, 1998; Van Heijst et al., 2001) and the Rio Grande (Banfield, 1998) deltas, and results from this investigation

and previous investigations (Simms et al., 2006) that place the central Texas shoreline near its current location since the early Holocene. Based on results from Snow (1998), Van Heijst et al. (2001) and Abdulah et al. (2004), at *ca* 10 to *ca* 9 ka the Brazos-Colorado deltaic system extended up to *ca* 80 km seaward of the modern coastline and *ca* 80 km along the Texas coast. The *ca* 7 to *ca* 4 ka eastern Rio Grande delta extended *ca* 80 km along the coast and *ca* 20 to *ca* 40 km seaward of the modern coastline (Banfield, 1998; Morton & Winker, 1979; Price, 1954) (Figure 1). These major deltaic systems were separated by *ca* 200 km and an *ca* 100 km embayment on the coast (Figure 1).

In modelling, the shoreface is delineated using a constant depth of closure D_c of −10 m (i.e. ravinement depth) below sea level, which is a reasonable estimate for the central Texas coast based on the alongshore depth of the furthest seaward extent of shoreface deposits (Rodriguez et al., 2001). Additionally, it is assumed that shoreline motion also reworks modest coastal topography, characterised by a height H of 2 m above sea level. This modelling strategy vastly minimises the complexity in simulating the generation of subaerial barrier topography, however, the selected height approximates Holocene beach ridge elevation (*ca* + 2.5 m above sea level; Blum & Carter, 2000), and therefore, in the following simulations shoreline motion is conceptually assumed to drive, or create, or destroy a beach ridge plain. In total, simulated shoreline motion occurs due to the motion of a uniform cross-shore profile of total width $D_p = D_c + H = 12$ m.

Because the wave climate along the ancient Texas coast is unknown, wave information from a multi-decadal hindcast simulation (Wave Information Studies, 2018) of the modern Texas coast (McGowen et al., 1977; Rodriguez et al., 2001) is used to frame three model cases which correspond to the 25th, 50th and 75th cumulative percentiles of wave height and wave period. Conceptually, these model cases provide a range of hypothetical wave climates that range from a very tranquil system (25th percentile) to very energetic (75th cumulative percentile) compared to the modern Texas coast. The three-wave classes used in the following simulations are deep water wave heights H_s of 0.51, 0.79 and 1.16 m and deep water wave periods T_s of 4.1, 4.7 and 5.5 s, for the 25th, 50th and 75th cumulative percentiles, respectively. These wave cases are probably conservative estimates as during the time period of interest the slightly more seaward shoreline position, and thus reduction of shelf width, may have allowed more wave energy to rework the ancient Brazos-Colorado (Snow, 1998) and Rio Grande deltaic headlands. For simplicity, it is assumed that each deep water wave class is applied uniformly across the simulated coastal system.

Following conventional longshore sediment transport modelling practices, in each modelled scenario, uniform trains of waves are assumed to refract, shoal and break at an angle equivalent to the slope of the shoreline (i.e. $\frac{dy}{dx}$) where x and y are the longshore and cross-shore shoreline coordinates, respectively. Longshore sediment transport is treated as a diffusive process (Ashton & Murray, 2006; Cooper & Pilkey, 2004; Larson et al., 1987; Pelnard-Considère, 1956; Ravens & Sitanggang, 2007; Rogers & Ravens, 2008), and shoreline diffusivity γ, approximated using deep water wave information by $\gamma = K_1 \left(\frac{\sqrt{g\gamma_b}}{2\pi} \right) H_s^{12/5} T_s^{1/5}$, where K_1 is a coefficient set to 0.4 $m^{1/2}/s$ to represent quartz sediment, γ_b is the wave breaking criterion ($\gamma_b = 0.78$); additionally, g is gravitational acceleration (9.806 m/s^2). Following the pioneering work of Komar (1971; 1973), the sediment flux imparted by longshore sediment transport q, is given as $q = -\frac{\gamma}{D_p}\frac{dy}{dx}$, and shoreline position change $\frac{dy}{dt}$, is calculated by conservation of sediment, $\frac{dy}{dt} = -\frac{dq}{dx}$. By combining these statements, a shoreline evolution equation is found, $\frac{dy}{dt} = \frac{\gamma}{Dp}\frac{d^2y}{dx^2}$. To account for shoreline motion due to inundation from sea-level rise, the entire littoral system is assumed to retreat landward at a constant rate $r = -1.63$ m/yr, given by the average rate of sea-level rise during the simulation period (1.6 mm/yr; Figure 7) and the average shelf slope of the study region (9.81×10^{-4}, NOAA Coastal Relief Model), which nearly matches the subaerial slope of the coastal plain (LeBlanc & Hodgson, 1959). The final form of the shoreline evolution equation is discretized using an explicit in time central differencing scheme, $y_{j+1} = y_j + dt\frac{\gamma}{D_p}\left(\frac{y_{i+1} + y_{i-1} - 2y_i}{dx^2}\right) + r dt$, where i and j represent discrete steps in space and time, respectively. During a

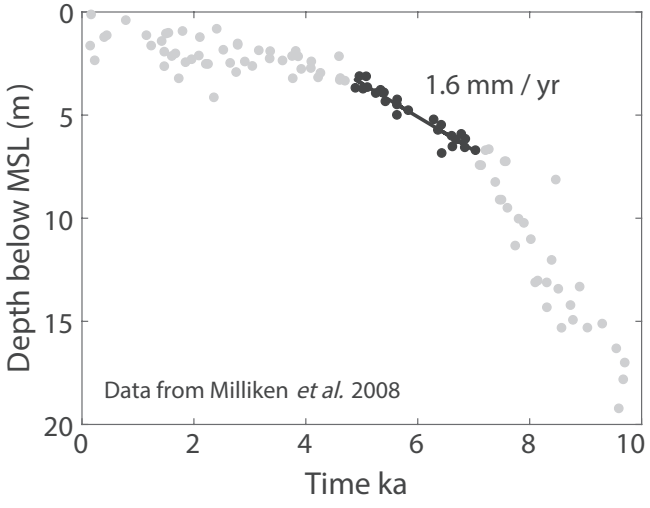

FIGURE 7 A) Simplified sea-level curve redrafted from Milliken et al. (2008). Solid black dots correspond to data within the simulation time (7,095–4,850 cal BP). Grey dots indicate data outside of the computer simulation

simulation, timesteps *dt* are held constant at 0.1 yr, and the total simulation time 2,245 yr, is constrained by differencing the average of the earliest and latest known dates for the onset of shoreface progradation (7,340 ± 25 cal BP and 6,450 ± 25 cal BP) and the onset of shoreface retreat (4,850 cal BP). The model domain is composed of 200 nodes with a uniform cell width *dx* of just under 2 km. Laterally, the domain extends from the ancient Brazos-Colorado to the Rio Grande deltas (Figure 8). At the northernmost edge of the model domain (alongshore distance km = 0, Figure 8), palaeogeographic reconstructions of the Brazos-Colorado Delta suggest that the *ca* 10 ka shoreline and *ca* 5 ka shoreline are at approximately the same position on the northern flank of the Brazos-Colorado Delta. Therefore, the shoreline position at the northernmost boundary is specified and held constant during model time steps (Dirichlet-type boundary condition). This boundary condition implies that sediment was supplied from either updrift regions, offshore sources, the Brazos and/or Colorado Rivers, or a combination thereof. Although the sediment source is unknown, until *ca* 5 ka, the Colorado River has been interpreted to discharge significantly more sediment compared to fluxes during the last millennium (Blum et al., 1994). However, a zero-flux boundary condition is applied at the Rio Grande Delta (alongshore km *ca* 348, Figure 8). This boundary condition forces the compartmentalisation of littoral transport to a single zone along the central portion of the Texas coast, which is reasonable given the orientation of the assumed wave climate and the prominence of the Rio Grande Delta compared to the more landward shoreline position to the north and south (Figure 1).

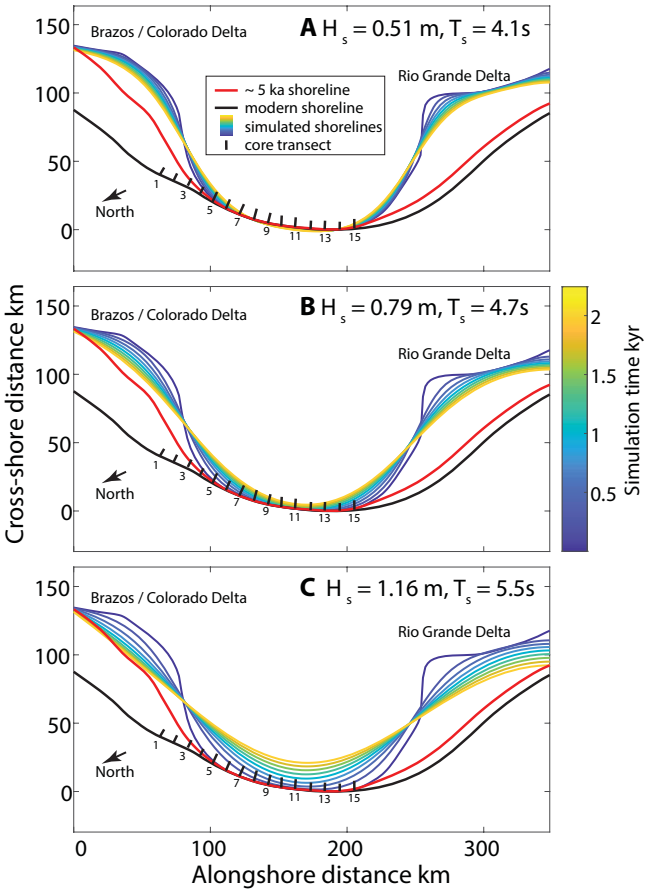

FIGURE 8 Selected times-steps of shoreline evolution (colour-mapped shoreline plotted every 250 yr). The first (darkest blue) shoreline is the reconstructed ancient shoreline (Banfield, 1998; Snow, 1998). (A) 25th percentile wave class: $H_s = 0.51$ m, $T_s = 4.1$ s, (B) Median wave class: $H_s = 0.79$ m, $T_s = 4.7$ s and (C) 75th percentile wave class:$H_s = 1.16$ m, $T_s = 5.5$ s. The solid black line in each plot is the modern shoreline of the study area (Paine et al., 2016). Core transect locations are indicated by the numbering of odd core transect locations

At the beginning of each simulation, sediment is quickly redistributed from the tip of both deltaic regions towards the sides (Figure 8). This lateral redistribution of sediment broadens the deltas and reduces shoreline curvature, which, in turn, reduces rates of shoreline change (Figures 8 and 9) and longshore sediment transport (Figure 10). Because each simulation is initialised using the same reconstructed shoreline, the specific wave class defines the rate at which each simulated shoreline evolves (Figure 8). Although all three simulations drive sediment transport towards the central Texas coast, the weakest wave climate (25th percentile, Figure 8A) is unable to offset shoreline retreat due to sea-level rise along much of the study area where shoreface progradation is observed (See Region between core transects 7 and 14 in Figure 8A). Along core transects 11 through 15, this wave forcing drives modest retreat (*ca* 1–2 km) for transects 11 through 13 (Figure 9A through C), and modest progradation for core transects 14 (*ca* 1 km) and 15 (*ca* 3.6 km; Figure 9D,E). In contrast, the median wave class can drive significant shoreline progradation along all core transects (Figure 8B). Although the median wave climate it is unable to force progradation beyond 4.4 km near core transect 11, where progradation in excess of 5 km is observed (Figures 6A and 9A), simulated progradation is in excess of 5 km for core transects 12 through 15 (Figure 9B through E). The 75th percentile wave class causes rapid shoreline progradation along all core transects and ravinement of nearly the entire Rio Grande Delta to roughly match the *ca* 5 ka reconstructed shoreline (Figure 8C). The least progradation occurs near Transect 11 (*ca* 22 km, Figure 9A) and the most progradation occurs near transect 15 (*ca* 28 km, Figure 9B). The simulated shoreline change involves a gross final redistribution of 29.1 km^3 (25th percentile wave class), 58.2 km^3 (median wave class) and 98.9 km^3 (75th percentile wave class) of shoreface materials (Figure 10).

This longshore transport model is uncalibrated and only informed by reasonable estimates of shoreline shape and possible wave climate of the ancient coastal system. Therefore, the results of these simulations are best viewed as a conceptual hypothesis check to see if reasonable wave climate

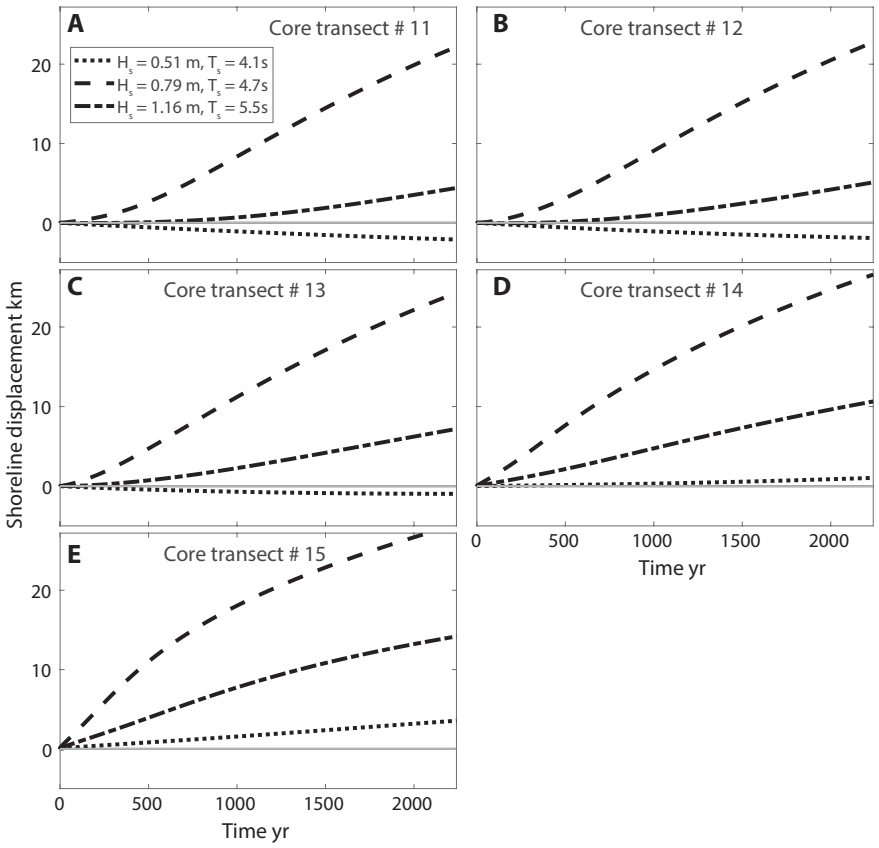

FIGURE 9 Shoreline displacement from the initial shoreline position at the alongshore position of core transects (A) 11, (B) 12, (C) 13, (D) 14, (E) 15. See Figures 2 and 11 for core transect locations

and shoreline shape are a reasonable mechanism to drive longshore convergence and shoreline progradation during a time of slow, but overall sea-level rise (Figure 7). Indeed, both the 50th and 75th cumulative percentiles wave height and period drive significant progradation across the study area (Figure 8B,C). However, conclusions drawn from these simulations must be tempered by the model's simplicity and incomplete description of physical processes that may have forced shoreline motion along the ancient Texas coast.

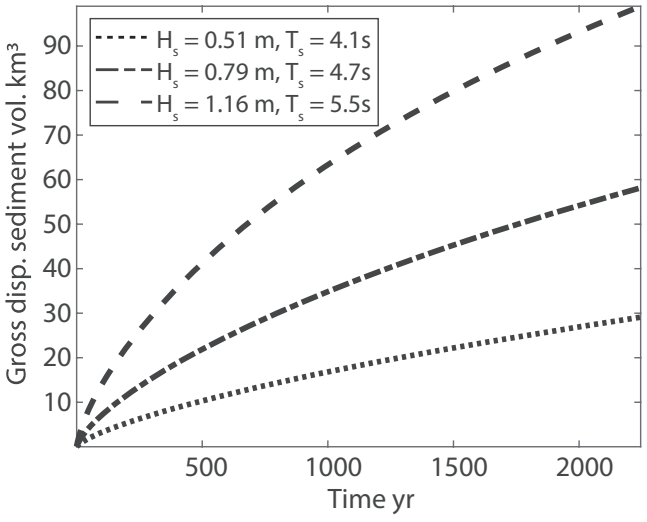

FIGURE 10 Gross displaced sediment volume (eroded and deposited) plotted as a function of simulation time for the three simulated wave classes

5 | DISCUSSION

While the long-term landward migration of the coast during the Late Pleistocene and Holocene was regulated by sea-level rise, core data from offshore central Texas indicate that the shoreface, and presumably the coastline, prograded and retrograded several kilometres during the Holocene as the rate of sea-level rise decreased.

During the early Holocene, an embayment existed along the central Texas coast that was flanked to the north and south by the Colorado and Rio Grande deltas, respectively (Figure 1). Both deltas changed from lobate, fluvial-dominated deltas to elongate, shore-aligned, wave-dominated deltas around 9.5 ka. This was followed by abandonment and reworking of these deltas, resulting in an increase in sand supply to the central Texas coast. Analysis of the sediment budget indicates that erosion of the Colorado and Rio Grande deltas could have yielded as much as 36.6 km^3 of sand to the central Texas coast, which is roughly equal to the total amount of sand that composes the modern central Texas barrier island system and the sand that is estimated to reside within Holocene shoreface and offshore storm deposits.

Radiocarbon dates, combined with results from previous studies, indicate that tidal delta growth and shoreface progradation was underway from *ca* 7.3 to *ca* 6.5 ka, this was approximately the time that sea-level rise decreased from an average rate of 4.1 mm/yr, punctuated by episodes of a rapid rise in excess of 10.0 mm/yr, to an average rate of rise of 1.6 mm/yr (Figure 7). Therefore, a reasonable supposition would be that as rates of sea-level rise slowed, shoreface sediment removal by offshore transport, barrier aggradation, overwash, or otherwise, also slowed. These changes are thought to have allowed longshore transport from the Brazos/Colorado and Rio Grande Deltas to nourish the central Texas coast, and drive shoreface progradation during this time.

Although wave climate and exact palaeo-shoreline shape during the Holocene are unknown quantities, within a reasonable range of wave climate and given an initial shoreline shape solely constructed using the well-established scales and locations of ancient delta complexes there are multiple lines of support to further explain the early-middle Holocene episode of shoreline progradation. First, the shape and orientation of the palaeo-shoreline would allow a broad range of wave approaches from the south-east to drive longshore sediment transport and convergence in the study area (boxed region, Figure 1). Second, simulations of shoreline motion driven by highly conservative values obtained from modern wave climate yield shoreline progradation along the study area at rates and magnitudes that agree with progradation interpreted from core transects (Figures 5 and 6). Third, the range of estimated gross sediment fluxes imparted from ravinement of the Brazos-Colorado and Rio Grande deltaic systems is readily satisfied by the range of modelled scenarios (Figure 10). These lines of evidence conceptually support the interpretation that the observed early–middle Holocene progradation along the central Texas coast was a result of the process of longshore transport operating along a sinuous coastline.

The culmination of early–middle Holocene progradation is marked by a flooding surface that separates shoreface sands from overlying marine mud. Off Mustang and North Padre islands, this flooding surface extends *ca* 4 km landward from the point of maximum middle Holocene shoreface progradation (Figure 6). This transgressive event is potentially recorded by extensive and thick washover deposits observed in ground penetrating radar profiles across North Padre Island (Garrison et al., 2010). Radiocarbon ages from cores TR 15-104, TR14-95 and TR 13-89 indicate that this transgressive phase occurred between 4.850 and 1.560 ka, or over a period of *ca* 3,300 years. This was about the time the regional rate of sea-level rise in the western Gulf of Mexico decreased from an average rate of 1.6 mm/yr to an average rate of 0.5 mm/yr (Livsey & Simms, 2013; Milliken et al., 2008), and there is no evidence for a punctuated sea-level event that could have caused this change (Figure 7).

Beginning *ca* 3.5 ka, the TMB experienced significant expansion and accumulated *ca* 172 km^3 (2.86×10^{11} t) of sediment, accounting for 57% of its total volume (Weight et al., 2011). As the TMB expanded it buried both the Colorado and Rio Grande deltas (e.g. Figure 5), shutting down these sand sources. Furthermore, the profound difference in the TMB flux (49 km^3/1,000 year) compared to the progradation flux (*ca* 3.2 km^3/1,000 yr), implies that growth and expansion of the TMB contributed to the landward retreat of the shoreline in the late Holocene. A similar situation occurred off the Amazon-Guianas coast where Amazon mud blankets relict fluvial sand that would otherwise provide a source of sand for nourishing and stabilising the coast (Anthony et al., 2010; Kuehl et al., 1986). In addition, the high influx and the viscosity of mud-rich waters dampen and attenuate wave energy and force mud deposition even in moderate energy environments as the mud blanket dewaters and gets welded to the shoreline (Wells, 1983; Wells & Coleman, 1981). Other cases of thick mud deposition in moderate energy environments have been reported from the Valencia continental shelf (Maldonado et al., 1983), the Brazilian continental shelf (Kuehl et al., 1986), the Guiana continental shelf (Anthony et al., 2010; Gratiot et al., 2007), the Amazon continental shelf (Kineke & Sternberg, 1995; Kineke et al., 1996), the Yellow Sea (Lim et al., 2007), the Helgoland mud blanket of the North Sea (Hanebuth et al., 2015) and the *ca* 80 m thick Galicia mud belt on the Iberian shelf (Lantzsch et al., 2009).

Expansion of the TMB does appear to have directly influenced coastal sedimentation, but what controls the flux of mud to the study area over millennial time scales? Currently, the south-east wind-dominated alongshore transport and Coriolis effect, coupled with the Louisiana-Texas Coastal Current circulation patterns, control the transport of mud from the Mississippi River to central Texas (Sionneau et al., 2008; Weight et al., 2011). Thus, a change in these currents could have impacted coastal evolution in the study area. A recent review of Holocene palaeoclimate records for Texas by Wong et al. (2015) shows a shift from warm and dry to cool and wet conditions in west Texas at *ca* 3.5 ka, but a more ambiguous late Holocene palaeoclimate record exists for central Texas. Thus, the exact mechanism for the observed expansion of the TMB during the late Holocene remains problematic, but it is argued here that this significant episode of the coastal retreat was triggered by the expansion of the TMB.

Following the late Holocene transgressive event, there was another phase of shoreface progradation. Three radiocarbon ages from cores TR 11-76, TR 12-82 and TR 15-103 indicate that this latest phase of shoreface progradation began approximately 500 years ago and continues into the Modern. In support of this change, there is evidence that Matagorda

Island, San Jose Island, Mustang Island and North Padre Island all experienced aggradation and progradation between *ca* 2.0 and *ca* 0.9 ka (Anderson et al., 2014; Shideler, 1986; Wilkinson, 1975).

The latest phase of shoreface growth could also be explained by a decrease in TMB expansion allowing renewed alongshore and offshore sand transport, an increase in storm-related sand transport, an increase in fluvial sand delivery to the coast, or some combination of these three. Unfortunately, existing radiocarbon data do not allow us to determine if the TMB experienced any significant change during this time (Weight et al., 2011), nor are there any known climate or palaeoclimate events that would have resulted in a significant reduction in sediment delivery to the TMB at this time. There is no evidence for an increase in fluvial sand delivery to the coast from the Brazos, Colorado or Rio Grande rivers. In fact, sand from these rivers has been largely sequestered in their deltas and beaches downstream of these deltas have been sediment starved in recent times.

Hurricane Carla of 1963 and other major hurricanes are known to have transported sand several kilometres off the Texas coast (Goff, et al., 2010; 2019; Hayes, 1967; McGowen et al., 1970; Morton, 1981; 2002; Snedden et al., 1988). Clearly, offshore sand transport during storms has been an important process, but there is no evidence for an increase in storm frequency in the region during the late Holocene, although the sedimentary record of storm activity does not include the time interval of the most recent progradation (Wallace & Anderson, 2010). Furthermore, grain size analyses show that modern shoreface deposits are mainly composed of homogenous and well-sorted fine sand (Figure 3), similar to the mid-Holocene progradational sands, and there is no evidence for an increase in very fine sand in recent time in the lower shoreface and inner shelf cores.

Given these observations, it is not possible to identify the exact cause of the most recent shoreface progradation, but given that it appears to coincide with aggradation of central Texas coastal barriers it is possible that this progradation is associated with a healing phase of barrier evolution (i.e. a phase where shoreface sediments are reworked as the shoreface re-establishes its slope after transgression; Cattaneo & Steel, 2003; Posamentier & Allen, 1993) following the late Holocene transgressive event.

Historical shoreline change has been minimal along the central Texas coast, with an average retreat rate of −0.30 m/yr (Gibeaut et al., 2006; Paine et al., 2012). Assuming that shoreline and shoreface migrations occur at about the same rate over decadal to century time scales, this indicates that the latest phase of coastal progradation has ceased in historical time. This is consistent with observations from other previous studies of the north and south Texas coast that suggest an acceleration of coastal retreat in historical time (Anderson et al., 2014; Wallace & Anderson, 2013).

6 | CONCLUSION

While sea-level rise was the dominant control on the evolution of the central Texas coast during the late Pleistocene and early Holocene, sediment supply, both across shore and onshore, resulted in two episodes of significant shoreface progradation and retrogradation as the rate of sea-level rise decreased during the middle-late Holocene. Radiocarbon ages indicate that the older episode of progradation was underway by *ca* 6.5 ka and ended *ca* 5 ka with nearly 5 km of shoreface progradation. Sediment budget calculations and sediment transport modelling results indicate that this progradation was the result of increased sand supply from erosion of the offshore Colorado and Rio Grande deltas.

A transgressive phase occurred between *ca* 4.9 and *ca* 1.6 ka and resulted in *ca* 4 km of landward shoreface migration. This marine flooding event coincided with the expansion of the TMB and associated burial of offshore sand sources. A more recent episode of shoreface progradation began *ca* 500 years ago and appears to have ended in historical time. The exact cause of this recent shoreface progradation remains uncertain, but it is believed to be a healing phase from the late Holocene transgressive event. During this event, the shoreface prograded at an average rate of *ca* 6 m/yr, compared to the historical rate of shoreline change of −0.30 m/yr. So, similar to other parts of the Texas coast, the current rate of change for central Texas appears to indicate a return to transgressive conditions.

DATA AVAILABILITY STATEMENT

All data generated or analysed during this study are available from the authors by reasonable request.

ORCID

Christopher I. Odezulu https://orcid.org/0000-0002-8034-6903
Travis Swanson https://orcid.org/0000-0002-6879-7621
John B. Anderson https://orcid.org/0000-0002-3104-5557

REFERENCES

Abdulah, K.C., Anderson, J.B., Snow, J.N. & Holdford-Jack, L. (2004). The Late Quaternary Brazos and Colorado Deltas, Offshore Texas, U.S.A.—Their evolution and the factors that controlled their deposition. In: Anderson, J.B. & Fillon, R.H. (Eds.), *Late Quaternary stratigraphic evolution of the Northern Gulf of Mexico Margin. SEPM Special Publication*, *79*, 237–269.

Anderson, J.B., Wallace, D.J., Simms, A.R., Rodriguez, A.B. & Milliken, K.T. (2014) Variable response of coastal environments of the northwestern Gulf of Mexico to sea-level rise and climate change: Implications for future change. *Marine Geology*, *352*, 348–366. https://doi.org/10.1016/j.margeo.2013.12.008

Anthony, E.J., Gardel, A., Gratiot, N., Proisy, C., Allison, M.A., Dolique, F. et al. (2010) The Amazon-influenced muddy coast

of South America: a review of mud-bank–shoreline interactions. *Earth-Science Reviews*, *103*(3), 99–121. https://doi.org/10.1016/j.earscirev.2010.09.008

Ashton, A.D. & Murray, A.B. (2006) High-angle wave instability and emergent shoreline shapes: 1. Modeling of sand waves, flying spits, and capes. *Journal of Geophysical Research: Earth Surface*, *111*(F4), https://doi.org/10.1029/2005JF000422

Banfield, L.A. (1998) Late Quaternary Evolution of the Rio Grande system, offshore south Texas. PhD thesis. Rice University.

Banfield, L.A. & Anderson, J.B. (2004). Late Quaternary evolution of the Rio Grande Delta: complex response to Eustasy and climate change. In: Anderson, J.B. & Fillon, R.H. (Eds.), *Late Quaternary stratigraphic evolution of the Northern Gulf of Mexico margin* (vol. 79). Tulsa, OK: SEPM Society for Sedimentary Geology. doi: 10.2110/pec.04.79.0289.

Blum, M.D. & Carter, A.E. (2000) Middle Holocene evolution of the Central Texas Coast. *GCAGS Transactions*, *50*, 331–341.

Blum, M.D., Toomey, R.S. & Valastro, S. (1994) Fluvial response to Late Quaternary climatic and environmental change, Edwards Plateau, Texas. *Palaeogeography, Palaeoclimatology, Palaeoecology*, *108*(1), 1–21. https://doi.org/10.1016/0031-0182(94)90019-1

Cattaneo, A. & Steel, R.J. (2003) Transgressive deposits: a review of their variability. *Earth-Science Reviews*, *62*(3–4), 187–228.

Cooper, J. & Pilkey, O.H.(2004) Longshore drift: trapped in an expected universe. *Journal of Sedimentary Research*, *74*(5), 599–606. https://doi.org/10.1306/022204740599

Curray, J.R. (1960) Sediments and history of Holocene transgression, continental shelf. *Northwest Gulf of Mexico*, *143*, 221–266.

Eckles, B.J., Fassell, M.L. & Anderson, J.B. (2004). Late Quaternary evolution of the wave–storm-dominated central Texas shelf. In: Anderson, J.B. & Fillon, R.H. (Eds.), *Late Quaternary stratigraphic evolution of the northern Gulf of Mexico Margin* (vol. 79). Tulsa, OK: SEPM Society for Sedimentary Geology. doi: 10.2110/pec.04.79.0271.

Fassell, M.L. (1999) Late Quaternary marine deposits, offshore central Texas: Processes controlling geometry, distribution, and preservation potential, Thesis. Rice University. https://scholarship.rice.edu/handle/1911/17263

Garrison, J.R., Williams, J., Miller, S.P., Weber, E.T., McMechan, G. & Zeng, X. (2010) Ground-penetrating radar study of North Padre Island: Implications for barrier island internal architecture, model for growth of progradational microtidal barrier Islands, and Gulf of Mexico sea-level cyclicity. *Journal of Sedimentary Research*, *80*(4), 303–319. https://doi.org/10.2110/jsr.2010.034

Gibeaut, J.C., Gutierrez, R., Waldinger, R., White, W.A., Hepner, T.L., Smyth, R.C.et al. (2006) The Texas shoreline change project. Gulf of Mexico Shoreline Change from the Brazos River to Pass Cavallo.

Goff, J.A., Allison, M.A. & Gulick, S.P. (2010) Offshore transport of sediment during cyclonic storms: Hurricane Ike (2008), Texas Gulf Coast, USA. *Geology*, *38*(4), 351–354.

Goff, J.A., Swartz, J.M., Gulick, S.P., Dawson, C.N. & de Alegria-Arzaburu, A.R. (2019) An outflow event on the left side of Hurricane Harvey: Erosion of barrier sand and seaward transport through Aransas Pass, Texas. *Geomorphology*, *334*, 44–57.

Gratiot, N., Gardel, A. & Anthony, E.J. (2007) Trade-wind waves and mud dynamics on the French Guiana coast, South America: Input from ERA-40 wave data and field investigations. *Marine Geology*, *236*(1), 15–26. https://doi.org/10.1016/j.margeo.2006.09.013

Hanebuth, T.J.J., Lantzsch, H. & Nizou, J. (2015) Mud depocenters on continental shelves—appearance, initiation times, and growth dynamics. *Geo-Marine Letters*, *35*(6), 487–503. https://doi.org/10.1007/s00367-015-0422-6

Hayes, M.O. (1967) Hurricanes as geological agents, South Texas Coast: Geological notes. *AAPG Bulletin*, *51*(6), 937–942.

Khanna, P., Droxler, A.W., Nittrouer, J.A. & Thunnell, J.W. and Shirley, T.C.(2017) Coralgal reef morphology records punctuated sea-level rise during the last deglaciation. *Nature Communications*, *8*(1), https://doi.org/10.1038/s41467-017-00966-x

Kineke, G.C. & Sternberg, R.W. (1995) Distribution of fluid muds on the Amazon continental shelf. *Marine Geology*, *125*(3), 193–233. https://doi.org/10.1016/0025-3227(95)00013-O

Kineke, G.C., Sternberg, R.W., Trowbridge, J.H. & Geyer, W.R. (1996) Fluid-mud processes on the Amazon continental shelf. *Continental Shelf Research*, *16*(5), 667–696. https://doi.org/10.1016/0278-4343(95)00050-X

Kolker, A.S., Allison, M.A. & Hameed, S. (2011) An evaluation of subsidence rates and sea-level variability in the northern Gulf of Mexico. *Geophysical Research Letters*, *38*(21), https://doi.org/10.1029/2011GL049458

Komar, P. (1971) The mechanics of sand transport on beaches. *Journal of Geophysical Research*, *76*(3), 713–721. https://doi.org/10.1029/JC076i003p00713

Komar, P.D. (1973) Computer models of delta growth due to sediment input from rivers and longshore transport. *GSA Bulletin*, *84*(7), 2217–2226. https://doi.org/10.1130/0016-7606(1973)84<2217:C-MODGD>2.0.CO;2

Kuehl, S.A., DeMaster, D.J. & Nittrouer, C.A. (1986) Nature of sediment accumulation on the Amazon continental shelf. *Continental Shelf Research*, *6*(1), 209–225. https://doi.org/10.1016/0278-4343(86)90061-0

Lantzsch, H., Hanebuth, T.J.J. & Bender, V.B. (2009) Holocene evolution of mud depocentres on a high-energy, low-accumulation shelf (NW Iberia). *Quaternary Research*, *72*(3), 325–336. https://doi.org/10.1016/j.yqres.2009.07.009

Larson, M., Hanson, H. & Kraus, N.C. (1987). Analytical solutions of the one-line model of shoreline change. Coastal Engineering Research Center, Vicksburg, MS.

LeBlanc, R.J. & Hodgson, W. (1959) Origin and development of the Texas shoreline. *Gulf Coast Association of Geological Societies Transactions*, *9*, 197–220.

Lim, D.I., Choi, J.Y., Jung, H.S., Rho, K.C. & Ahn, K.S. (2007) Recent sediment accumulation and origin of shelf mud deposits in the Yellow and East China Seas. *Progress in Oceanography*, *73*(2), 145–159. https://doi.org/10.1016/j.pocean.2007.02.004

Livsey, D. & Simms, A.R. (2013) Holocene sea-level change derived from microbial mats. *Geology*, *41*(9), 971–974. https://doi.org/10.1130/G34387.1

Lohse, E.A. (1955). Dynamic Geology of the Modern Coastal Region, Northwest Gulf of Mexico. In Hough, J.L. & Menard, H.W. (Eds.), vol. 3. Society of Economic Paleontologists and Mineralogists Special Publication. pp. 99–105. http://archives.datapages.com/data/sepm_sp/SP3/Dynamic_Geology.htm

Maddox, J., Anderson, J.B., Milliken, K.T., Rodriguez, A.B., Dellapenna, T.M. & Giosan, L. (2008) The Holocene evolution of the Matagorda and Lavaca estuary complex, Texas, USA. *Response of Gulf Coast estuaries to sea-level rise and climate change*. Geological Society of America, Special Paper 443, 105–119.

Maldonado, A., Swift, D.J.P., Young, R.A., Han, G., Nittrouer, C.A., DeMaster, D.J. et al. (1983) Sedimentation on the valencia continental shelf: Preliminary results. *Continental Shelf Research*, *2*(2), 195–211. https://doi.org/10.1016/0278-4343(83)90016-X

McGowen, J.H., Garner, L.E. & Wilkinson, B.H. (1977) The Gulf shoreline of Texas: processes, characteristics, and factors in use. https://repositories.tdl.org/tamug-ir/handle/1969.3/19988

McGowen, J.H., Groat, C.G., Brown, L.F. Jr, Fisher, W.L. & Scott, A.J. (1970) Effects of Hurricane Celia, a focus on environmental geologic problems of the Texas coastal zone. University of Texas at Austin, Bureau of Economic Geology.

Milliken, K.T., Anderson, J.B. & Rodriguez, A.B. (2008) A new composite Holocene sea-level curve for the northern Gulf of Mexico. *Geological Society of America Special Paper*, *443*, 1–11.

Morton, R.A. (1977) Historical shoreline changes and their causes, Texas Gulf Coast. *Gulf Coast Association of Geological Societies Transactions*, *27*, 352–364.

Morton, R.A. (1981) Formation of storm deposits by wind-forced currents in the Gulf of Mexico and the North Sea. In *Holocene marine sedimentation in the North Sea Basin*. 5. New York: International Association of Sedimentologists, pp. 385–396.

Morton, R.A. (2002). Factors controlling storm impacts on coastal barriers and beaches: A preliminary basis for near real-time forecasting. *Journal of Coastal Research*, *18*(3), 486–501. JSTOR.

Morton, R.A., Bernier, J.C. & Barras, J.A. (2006) Evidence of regional subsidence and associated interior wetland loss induced by hydrocarbon production, Gulf Coast region, USA. *Environmental Geology*, *50*(2), 261. https://doi.org/10.1007/s00254-006-0207-3

Morton, R.A., Miller, T.L. & Moore, L.J. (2004) National assessment of shoreline change: Part 1 Historical shoreline changes and associated coastal land loss along the US Gulf of Mexico. US Geological Survey.

Morton, R.A. & Winker, C.D. (1979) Distribution and Significance of coarse biogenic and clastic deposits on the Texas inner shelf (1). *Gulf Coast Association of Geological Societies Transactions*, *29*, 306–320.

NOAA Tides and Currents (2012). https://tidesandcurrents.noaa.gov/

Odezulu, C.I., Lorenzo-Trueba, J., Wallace, D.J. & Anderson, J.B. (2018) Follets Island: A case of unprecedented change and transition from rollover to subaqueous shoals. *Barrier dynamics and response to changing climate*. Cham, Switzerland: Springer, pp. 147–174.

Otvos, E.G. & Howat, W.E. (1996) South Texas Ingleside Barrier: Coastal sediment cycles and vertebrate Fauna. Late Pleistocene stratigraphy revised. *Gulf Coast Association of Geological Societies Transactions*, *46*, 333–344.

Paine, J.G. (1993) Subsidence of the Texas coast: Inferences from historical and late Pleistocene sea levels. *Tectonophysics*, *222*(3), 445–458. https://doi.org/10.1016/0040-1951(93)90363-O

Paine, J.G., Caudle, T.L. & Andrews, J.R. (2016) Shoreline and sand storage dynamics from annual airborne LIDAR Surveys, Texas Gulf Coast. *Journal of Coastal Research*, *333*, 487–506. https://doi.org/10.2112/JCOASTRES-D-15-00241.1

Paine, J.G., Mathew, S. & Caudle, T. (2012) Historical shoreline change through 2007, Texas Gulf Coast: Rates, contributing causes, and Holocene context. *Gulf Coast Association of Geological Societies Journal*, *1*, 13–26.

Pelnard-Considère, R. (1956). Essai de théorie de l'évolution des formes de rivage en plages de sable et de galets. Les Energies de La Mer: Compte Rendu Des Quatriemes Journees de L'hydraulique, Paris 13, 14 and 15 Juin 1956; Question III, Rapport 1, 74–1-10. http://resolver.tudelft.nl/uuid:c6e1ce87-23ef-4a3d-86d0-47f3c96518cc.

Posamentier, H.W. & Allen, G.P. (1993) Siliciclastic sequence stratigraphic patterns in foreland, ramp-type basins. *Geology*, *21*(5), 455–458.

Price, W.A. (1954). Dynamic environments: reconnaissance mapping, geologic and geomorphic, of continental shelf of Gulf of Mexico. *Gulf Coast Association of Geological Societies Transactions*, *4*, 75–107.

Ravens, T.M. & Sitanggang, K.I. (2007) Numerical modeling and analysis of shoreline change on Galveston Island. *Journal of Coastal Research*, *233*, 699–710. https://doi.org/10.2112/04-0191.1

Reimer, P.J., Bard, E., Bayliss, A., Beck, J.W., Blackwell, P.G., Ramsey, C.B. et al. (2013) IntCal13 and marine13 radiocarbon age calibration curves 0–50,000 years cal BP. *Radiocarbon*, *55*(4), 1869–1887. https://doi.org/10.2458/azu_js_rc.55.16947

Rodriguez, A.B., Fassell, M.L. & Anderson, J.B. (2001) Variations in shoreface progradation and ravinement along the Texas coast, Gulf of Mexico. *Sedimentology*, *48*(4), 837–853. https://doi.org/10.1046/j.1365-3091.2001.00390.x

Rogers, A.L. & Ravens, T.M. (2008) Measurement of longshore sediment transport rates in the surf zone on Galveston Island, Texas. *Journal of Coastal Research*, *24*(2B), 62–73.

Shideler, G.L. (1978) A sediment-dispersal model for the South Texas continental shelf, northwest Gulf of Mexico. *Marine Geology*, *26*(3), 289–313. https://doi.org/10.1016/0025-3227(78)90064-6

Shideler, G.L. (1986). Stratigraphic studies of a late Quaternary barrier-type coastal complex, Mustang Island-Corpus Christi Bay area, South Texas Gulf Coast (Report No. 1328; Professional Paper). USGS Publications Warehouse. doi: 10.3133/pp1328.

Simms, A.R., Anderson, J.B. & Blum, M. (2006) Barrier-island aggradation via inlet migration: Mustang Island, Texas. *Sedimentary Geology*, *187*(1), 105–125. https://doi.org/10.1016/j.sedgeo.2005.12.023

Simms, A.R., Anderson, J.B., DeWitt, R., Lambeck, K. & Purcell, A. (2013) Quantifying rates of coastal subsidence since the last interglacial and the role of sediment loading. *Global and Planetary Change*, *111*, 296–308. https://doi.org/10.1016/j.gloplacha.2013.10.002

Simms, A.R., Lambeck, K., Purcell, A., Anderson, J.B. & Rodriguez, A.B. (2007) Sea-level history of the Gulf of Mexico since the last glacial maximum with implications for the melting history of the Laurentide Ice Sheet. *Quaternary Science Reviews*, *26*(7), 920–940. https://doi.org/10.1016/j.quascirev.2007.01.001

Sionneau, T., Bout-Roumazeilles, V., Biscaye, P.E., Van Vliet-Lanoe, B. & Bory, A. (2008) Clay mineral distributions in and around the Mississippi River watershed and Northern Gulf of Mexico: sources and transport patterns. *Quaternary Science Reviews*, *27*(17), 1740–1751. https://doi.org/10.1016/j.quascirev.2008.07.001

Siringan, F.P. & Anderson, J.B. (1994) Modern shoreface and inner-shelf storm deposits off the east Texas coast, Gulf of Mexico. *Journal of Sedimentary Research*, *64*(2), 99–110.

Snedden, J.W., Nummedal, D. & Amos, A.F. (1988) Storm- and fair-weather combined flow on the central Texas continental shelf. *Journal of Sedimentary Research*, *58*(4), 580–595. https://doi.org/10.1306/212F8DFA-2B24-11D7-8648000102C1865D

Snow, J.N. (1998) Late Quaternary highstand and transgressive deltas of the ancestral Colorado River: eustatic and climatic controls on deposition, MA thesis. Rice University.

Van Heijst, M.W.I.M., Postma, G., Meijer, X.D., Snow, J.N. & Anderson, J.B. (2001) Quantitative analogue flume-model study of river-shelf

systems: principles and verification exemplified by the Late Quaternary Colorado river-delta evolution. *Basin Research*, *13*(3), 243–268.

Wallace, D.J. & Anderson, J.B. (2010) Evidence of similar probability of intense hurricane strikes for the Gulf of Mexico over the late Holocene. *Geology*, *38*(6), 511–514. https://doi.org/10.1130/G30729.1

Wallace, D.J. & Anderson, J.B. (2013) Unprecedented erosion of the upper Texas coast: Response to accelerated sea-level rise and hurricane impacts. *GSA Bulletin*, *125*(5–6), 728–740. https://doi.org/10.1130/B30725.1

Wave Information Studies. (2018). http://wis.usace.army.mil/

Weight, R.W.R., Anderson, J.B. & Fernandez, R. (2011) Rapid mud accumulation on the Central Texas shelf linked to climate change and sea-level rise. *Journal of Sedimentary Research*, *81*(10), 743–764. https://doi.org/10.2110/jsr.2011.57

Wells, J.T. (1983) Dynamics of coastal fluid muds in low-, moderate-, and high-tide-range environments. *Canadian Journal of Fisheries and Aquatic Sciences*, *40*(S1), s130–s142. https://doi.org/10.1139/f83-276

Wells, J.T. & Coleman, J.M. (1981) Physical processes and fine-grained sediment dynamics, coast of Surinam, South America. *Journal of Sedimentary Research*, *51*(4), 1053–1068. https://doi.org/10.1306/212F7E1E-2B24-11D7-8648000102C1865D

Wilkinson, B.H. (1975) Matagorda Island, Texas: The evolution of a gulf coast barrier complex. *GSA Bulletin*, *86*(7), 959–967. https://doi.org/10.1130/0016-7606(1975)86<959:MITTEO>2.0.CO;2

Wilkinson, B.H. & Basse, R.A. (1978) Late Holocene history of the Central Texas coast from Galveston Island to Pass Cavallo. *GSA Bulletin*, *89*(10), 1592–1600. https://doi.org/10.1130/0016-7606(1978)89<1592:LHHOTC>2.0.CO;2

Wilkinson, B.H. & McGowen, J.H. (1977) Geologic approaches to the determination of long-term coastal recession rates, Matagorda Peninsula, Texas. *Environmental Geology*, *1*(6), 359–365. https://doi.org/10.1007/BF02380504

Wong, C.I., Banner, J.L. & Musgrove, M. (2015) Holocene climate variability in Texas, USA: An integration of existing paleoclimate data and modeling with a new, high-resolution speleothem record. *Quaternary Science Reviews*, *127*, 155–173. https://doi.org/10.1016/j.quascirev.2015.06.023

How to cite this article: Odezulu CI, Swanson T, Anderson JB. Holocene progradation and retrogradation of the Central Texas Coast regulated by alongshore and cross-shore sediment flux variability. *Depositional Rec*. 2021;7:77–92. https://doi.org/10.1002/dep2.130